Journal of Applied Polymer Science

Supramolecular Thermoplastic Elastomer with Thermally Scratch Repairable Effect from 3-Amino-1,2,4-Triazole Crosslinked Maleated Polyethylene-Octene Elastomer/Nylon 12 Blends

Muhammad Kashif, Young-Wook Chang
Polymer Nano Materials Laboratory, Department of Chemical Engineering, Hanyang University, Ansan, Gyeonggi 426-791, Republic of Korea
Correspondence to: Y. W. Chang (E-mail: ywchang@hanyang.ac.kr)

ABSTRACT: In this study, nylon 12 (5–25 wt %) was melt blended with a supramolecular thermally repairable thermoplastic elastomer (ATA-POE), which was generated by crosslinking of maleated polyethylene-octene elastomer (mPOE) with 3-amino-1,2,4-triazole (ATA), in an internal mixer. The effect of nylon 12 content on the phase morphology, thermomechanical properties, and thermally triggered scratch repairing effects of the ATA-POE/nylon 12 blends was investigated. Scanning electron microscopy results showed that nylon 12 formed a dispersed phase with submicron scale in a continuous ATA-POE phase. Fourier transform infrared spectroscopy and differential scanning calorimetry analysis revealed that there are extensive hydrogen bonding interactions between the ATA-POE and nylon 12 in the blends, which was manifested by a decrease in the melting temperature of each polymer component. Tensile and dynamic mechanical test showed that tensile modulus increased with increasing nylon 12 contents in the blend with maintaining fairly high elastic recoverability. Furthermore, the blends containing up to 20 wt % of nylon 12 showed good scratch repairing effects when they are heated above melting temperature of the ATA-POE phase in the blend. © 2014 Wiley Periodicals, Inc. J. Appl. Polym. Sci. **2015**, *132*, 41511.

KEYWORDS: crosslinking; elastomers; mechanical properties; supramolecular structures; thermoplastics

Received 14 June 2014; accepted 8 September 2014
DOI: 10.1002/app.41511

INTRODUCTION

Thermoplastic elastomers (TPEs) are important class of materials which combine the service properties of crosslinked elastomers at normal temperature and melt processing properties of thermoplastics at increased temperatures.[1] The market for TPEs is continuously growing because of their ability of recycling and reprocessing, and there are ongoing interests to develop the TPEs with high performance and functionalities to meet the demands for variety of applications.[2–4]

The crosslinks in these materials are thermoreversible hard domains which can be formed from phase separation, crystallization, ionic interactions, or hydrogen bonding interactions.[5–7] Various types of TPEs have been developed based on the concept. Segmented or block copolymer type TPEs are most representative ones in which semicrystalline or glassy phase form rigid domains below T_m or T_g of the hard segment within the soft polymer matrix.[8] Ionomeric TPEs are another type of TPEs in which small amount of ionic groups existed on the rubber chain form microphase-separated ionic aggregates that act as physical crosslinks.[9,10] TPEs based on reactive blending of nylons with maleated rubber have been also extensively studied in which rubber–graft–nylon copolymer is formed and provide synergistic properties to the blend.[11]

TPEs based on supramolecular hydrogen bonding interactions have been studied in recent years. Chino and Ashiura offered a simple way to prepare TPE comprising supramolecular hydrogen bonding network by the reactive melt mixing of maleated rubber with 3-amino-1,2,4-triazole (ATA).[12,13] Ring opening of maleic anhydride by amino group of ATA during the melt blending led to the formation of amide acids to cause thermoreversible supramolecular hydrogen bonded elastomer network. Peng and Abetz[14] reported on the preparation of supramolecular hydrogen-bonded thermoreversible crosslinked rubber by a series of chemical modification of polybutadiene (epoxidation, oxirane ring-opening, and sulfonyl isocyanate addition). Sun et al.[15] prepared a TPE using hydrogen bonding and ionic interactions by the reaction of maleated rubber with excess long chain alkyl amines. More recently, Chen et al.[16] developed a multiphase supramolecular TPE with self-healing capability. The designed hydrogen bonding brush polymers self-assemble into a hard–soft microphase-separated system, combining the

enhanced stiffness and toughness with the self-healing capability of dynamic supramolecular assemblies.

In our previous article,[17] we observed that crosslinking of maleated polyethylene–octene elastomer (mPOE) having small amount of crystallinity with 3-amino-1,2,4-triazole (ATA) can produce supramolecular TPE with thermally triggered scratch repairing ability as well as shape memory effect. It was thought that the scratch repairability of this TPE is attributed to both supramolecular hydrogen bonding interactions between the elastomer chains and shape memory effect.

In the present study, we observed that addition of a small amount of nylon 12 (less than 20 wt %) into the ATA-POE enhance mechanical properties of the ATA-POE with maintaining its scratch repairing ability. Intermolecular interactions between the ATA-POE and nylon 12 were investigated. Effects of nylon 12 content on the phase morphology, mechanical properties, and scratch repairing effects of the ATA-POE/nylon 12 blends were studied and the results are reported here.

EXPERIMENTAL

Materials

Semicrystalline mPOE (Amplify GR-216) having high maleic anhydride content (>0.5 wt %) was purchased from The Dow Chemical Company, USA. Nylon 12 (Rilsan AESNO TL) was purchased from Arkema ATA having melting point of 154–159°C was purchased from Tokyo Kasei Kogyo Co., Japan.

Sample Preparation

ATA-POE was prepared first by melt blending of mPOE with 10 phr of ATA at 180°C for 5 min in an internal mixer, as reported in our previous article.[17] Then, nylon 12 was melted for 2 min and ATA-POE was added. Mixing continued for 5 min with ATA-POE/nylon ratio of 95/5 (APN-5), 90/10 (APN-10), 85/15 (APN-15), 80/20 (APN-20), and 75/25 (APN-25) wt/wt, respectively. The blended samples were then molded as sheets at 180°C for 20 min using an electrically heated hydraulic press. The samples for different characterizations were punched out from this sheet.

Characterizations

Fourier transform infrared (FTIR) analysis was conducted by using Varian-800 FTIR spectrometer to study the possible hydrogen bonding interactions between ATA-POE and nylon 12. FTIR spectra were obtained at room temperature on thin film over a range of 650–4000 cm^{-1}.

The phase morphology of the ATA-POE/nylon 12 blend samples was recorded by field emission scanning electron microscopy (FE-SEM, JEOL JSM-630F) at an accelerating voltage of 15 kV. The samples were cryogenically fractured and nylon 12 phase is preferentially extracted by treating the blend samples in m-cresol overnight. The extracted samples were coated with thin layer of platinum.

Melting transitions of the blended samples were determined from differential scanning calorimeter (TA Instruments, DSC 2010). Blended samples were first heated from 30 to 200°C at a rate of 10°C min^{-1} under a nitrogen atmosphere and were then kept for 5 min at this temperature to remove prior thermal history. The samples were then cooled to −100°C at a rate of 10°C min^{-1} to determine the crystallization temperature (T_c). Subsequently, the samples were reheated to 200°C at a rate of 10°C min^{-1} to determine the melting temperature.

Dynamic mechanical analysis of the ATA-POE/nylon 12 blended samples were performed by using dynamic mechanical analyzer (TA instruments, model DMA 2980). The samples were subjected to cyclic tensile strain amplitude of 10 μm and frequency of 1 Hz. The temperature of the samples was increased from −100 to +200°C at a heating rate of 2°C min^{-1} in a liquid nitrogen atmosphere. The tension mode method was used to measure the storage modulus and tan δ values.

Tensile properties of the samples were determined by using universal testing machine Shimadzu (AGS-500NX) at 25°C and with a crosshead speed of 500 mm/min, according to ASTM D412 specifications. At least five dog-bone-shaped samples were used for characterization of each sample. Elastic moduli were determined from stress-strain curve of each sample at 1% strain. Elastic recoverability of the blended samples was determined from tension set values. Blended samples were stretched to 100% elongation and kept in this position for 10 min. The applied stress was then removed and the samples were kept for 10 min. Tension set was determined by the following formula:

$$\text{Tension set}(\%) = (\text{change in length}/\text{original length}) \times 100$$

FE-SEM (JEOL JSM-630F) was also used to study the thermal healing property. Initially, a scratch (60–70% of total thickness) was made on the samples and kept in the convection oven at 80°C for 5 min to check healing ability through FE-SEM. Healing efficiency of the blended sample (APN-10) was quantified in terms of tensile strength values. A scratch 60–70% of total thickness was made on the sample and kept in an oven for 2 h at 90°C. At least, three dog-bone-shaped samples were tested for healing.

RESULTS AND DISCUSSION

FTIR Spectroscopy

FTIR analysis was performed to examine the possible hydrogen bonding interactions between the ATA-POE and nylon 12. Figure 1 shows FTIR spectra of the neat ATA-POE, neat nylon 12, and ATA-POE/nylon 12 (80/20) blend. In the FTIR spectrum of neat ATA-POE, transmittance band at 1644 and 1526 cm^{-1} corresponds to amide and 1552 cm^{-1} corresponds to asymmetric stretching vibration of carboxylate group (—COO^-), can be seen.[17,18] The FTIR spectrum of ATA-POE/nylon 12 (80/20) blend shows that carbonyl group of amide is shifted from 1644 to 1640 cm^{-1} and carboxylate group peak at 1552 cm^{-1} submerged into strong peak of amide N—H stretching (1558 cm^{-1}) of nylon 12, in the blend because of hydrogen bonding interactions between ATA-POE and nylon 12. The other characteristic bands observed in the blend are at 3292 and 1162 cm^{-1}, which corresponds to hydrogen bonded —NH stretching and, CH_2 and CO—NH vibrations, respectively, which are not present in the spectrum of neat ATA-POE.[19] Indeed, nylon 12 shows —NH stretching and, CH_2 and CO—NH vibrations at 3288 and 1160 cm^{-1}, respectively. These

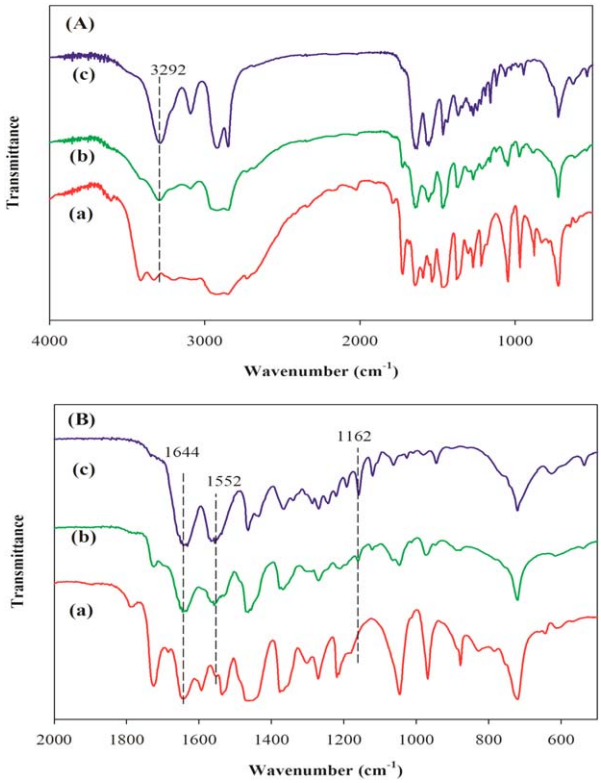

Figure 1. FTIR spectra of the (a) neat ATA-POE (b) ATA-POE/nylon 12 (80/20) blend and (c) neat nylon 12 from (A) 4000–500 cm^{-1} and from (B) 2000–500 cm^{-1}. [Color figure can be viewed in the online issue, which is available at wileyonlinelibrary.com.]

shifts in wavenumber (cm^{-1}) are attributed to hydrogen bonding interactions between the blended components. The proposed model for hydrogen bonding interactions between the supramolecular TPE (ATA-POE) and nylon 12 is shown in Figure 2.[17] This model intended to describe supramolecular hydrogen bonding and ionic interactions of the ATA-POE phase

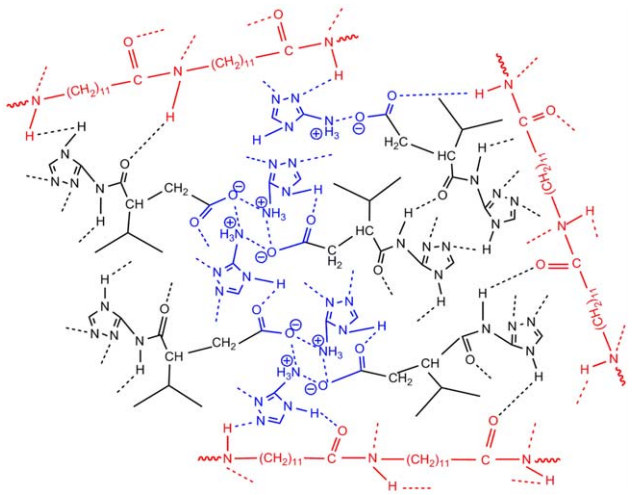

Figure 2. Speculative model for hydrogen bonding interactions between ATA-POE and nylon 12 blends. [Color figure can be viewed in the online issue, which is available at wileyonlinelibrary.com.]

undergo hydrogen bonding interactions with the amide group of nylon 12.

Phase Morphology

The phase morphology of the ATA-POE/nylon 12 blends was observed by field emission SEM micrographs and shown in Figure 3. The black spots in the micrographs represent dispersed nylon 12 phase which was preferentially extracted by m-cresol. It is certain that all the blends have phase-separated morphology, in which nylon 12 forms dispersed phase in the continuous ATA-POE matrix. Average domain size of the dispersed phase is about 200 nm in diameter in the blend with nylon 12 contents up to 5 wt %, and it increased to 700 nm with increasing nylon 12 contents up to 25 wt % in the blend. Randomly dispersed spherical particles of nylon 12 also showed elongated morphology at 20–25 wt % nylon 12 contents [Figure 3(e,f)] in the blends which is attributed to coalescence of nylon 12 particles. The extent of coalescence depends upon volume fraction of the dispersed phase, radius of particles, viscosity of each phase, and their interfacial tension.[20]

Differential Scanning Calorimetry

DSC measurements were performed to examine the thermal characteristics of the ATA-POE/nylon 12 blends and the results are summarized in Table I, which gives details about nonisothermal crystallization temperature (T_c), melting temperature (T_m), heat of fusion (ΔH_m), and associated degree of crystallinity (χ_c) for the elastomer phase. The degree of crystallinity of the elastomer phase in the blends were calculated using heat of fusion per gram of ATA-POE determined from DSC measurements and the heat of fusion corresponding to 100% crystalline LDPE (289 J g^{-1}).[21] Figure 4 shows second heating thermograms of neat ATA-POE, neat nylon 12, and ATA-POE/nylon 12 blends. Neat ATA-POE shows two endothermic peaks; one at around 60°C (T_m) related to melting transition of POE crystals and second at around 156°C (T_h) corresponds to melting temperature of free ATA, whereas mPOE has melting temperature of 63.7°C.[17] All the blends show another endothermic peak at around 163°C (T_n) due to the melting transition of nylon 12. The intensity of third peak relating to melting temperature of nylon 12 shows increasing trend with increase in nylon 12 contents in the blend.

Since melting temperature of free ATA and nylon 12 are very close to each other in the blends, only degree of crystallinity (χ_c) of POE was discussed. Table I show that the ΔH_m and T_c of the elastomer phase (ATA-POE) showing decreasing trend with increase in the nylon 12 content in the blends, whereas T_m shows marginal change. The hydrogen bonding interactions between the blended components restricted the molecular mobility of the POE chains and thus crystallization of the POE is restricted. As a consequence, the higher nylon 12 contents in the blends give rise to reduction in crystal size, which is manifested by slight decrease in T_m and χ_c.

The decrease in degree of crystallinity of the elastomer phase and a decrease in melting temperature of nylon 12 phase in the blends imply that there exist specific intermolecular interactions at the interfaces between the polymer components in the blends.[22,23] In the ATA-POE/nylon 12 (80/20) blend, the melting

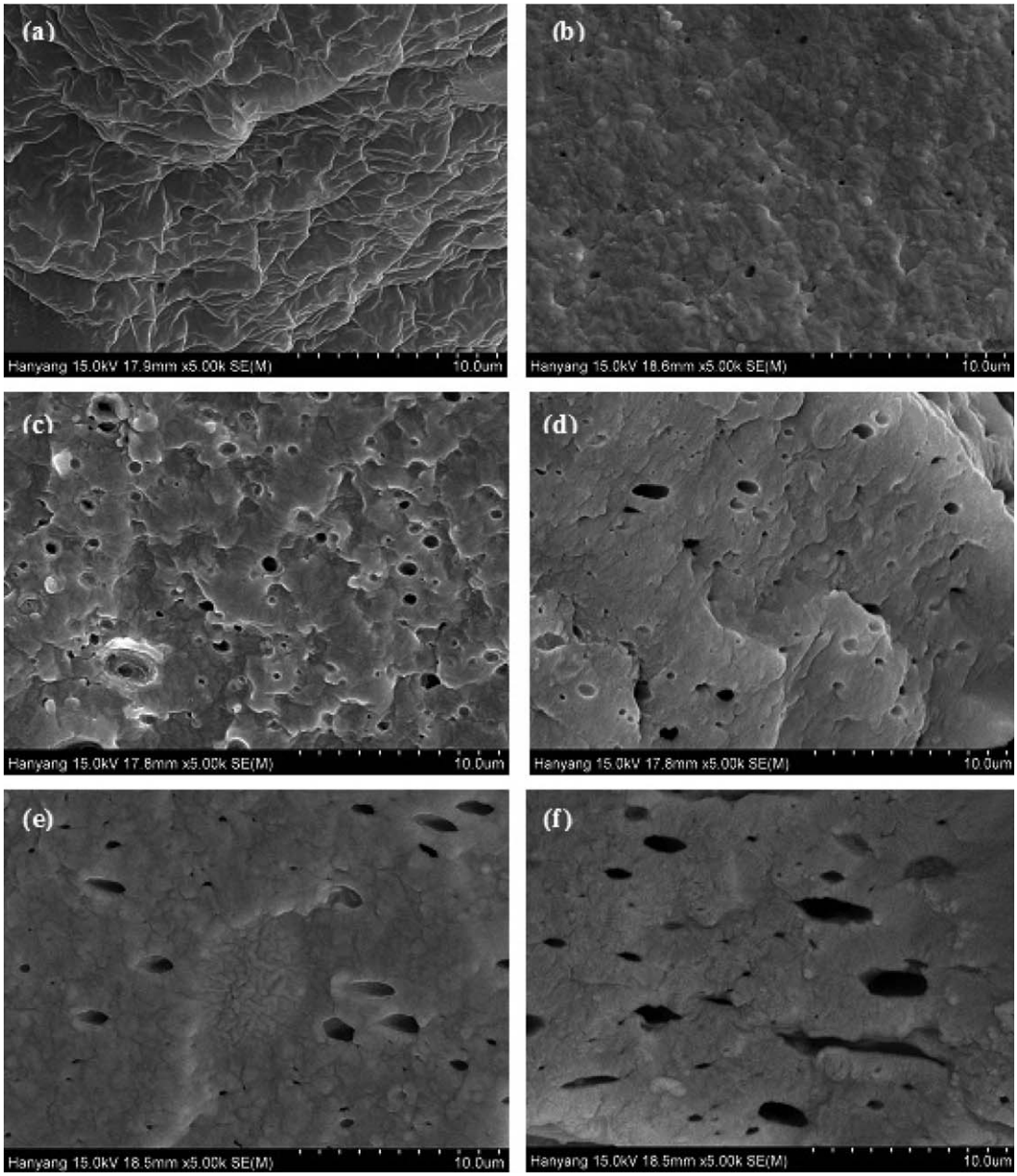

Figure 3. SEM micrographs of ATA-POE/Nylon 12 blends: (a) neat ATA-POE, (b) APN-5, (c) APN-10, (d) APN-15, (e) APN-20, and (f) APN-25.

temperature of nylon 12 decreased to 163.6°C from 178.4°C of neat nylon 12. It is well known that melting temperature of crystalline component is lowered as compared with neat polymer in the compatible blends. Herein, the decrease in the melting temperature of the elastomer phase is marginal, whereas significant decrease in the melting temperature of nylon 12 phase is observed in the blends with respect to neat nylon 12.

Dynamic Mechanical Analysis

Figure 5(a,b) represents the variation of storage modulus and tan δ as a function of temperature with increasing nylon 12 contents in the ATA-POE/nylon 12 blends, respectively. It is revealed from Figure 5(a) that storage modulus is increased with increasing nylon 12 contents in the blend at a temperature higher than 0°C. Table II provides storage modulus values at particular temperature with increasing nylon 12 contents in the blend. The storage modulus at 30°C, for example, is increased from 15.55 to 35 MPa when nylon 12 contents are raised from 0 to 25 wt % in the blend. This indicates that nylon 12 can increase the stiffness of the elastomer effectively.

Figure 5(b) shows variation of tan δ with respect to temperature and position of peak maximum corresponds to glass transition temperature (T_g) of the sample. The small increase in T_g was observed in the blends for the elastomer phase as the nylon 12 contents was increased in the blends. Hydrogen bonding interactions between the blended components at the interfaces reduces the chain mobility of the elastomer phase which is responsible for the increased T_g of the blends.

Table I. Thermal Characteristics of the ATA-POE/Nylon 12 Blends

Sample	ATA-POE				Nylon 12	
	T_c (°C)	T_m (°C)	ΔH_m (J g^{-1})	χ_c^a (%)	T_n (°C)	T_h (°C)
Neat Nylon 12	-	-	-	-	178.40	-
Neat ATA-POE	38.11	60.58	15.11	5.23	-	156.02
APN-5	36.95	59.92	13.86	4.99	163.10	156.05
APN-10	36.66	60.42	12.96	4.87	163.15	156.09
APN-15	36.34	60.22	12.36	4.86	163.46	156.09
APN-20	35.78	59.99	11.42	4.72	163.60	156.09
APN-25	34.39	59.42	10.34	4.51	164.10	156.09

$\chi_c^a = 100 \times (\Delta H_m/\Delta H^\circ_m)/w$, where ΔH°_m is heat of melting for 100% crystalline LDPE (289 J g^{-1}) and w is the weight fraction of ATA-POE phase in the blend.
T_c = crystallization temperature of ATA-POE, T_m = melting temperature of ATA-POE.
T_n = melting temperature of nylon 12, T_h = melting temperature of free ATA.

Tensile Properties

Stress–strain curves of the neat ATA-POE and ATA-POE/nylon 12 blends are shown in Figure 6. It can be seen that tensile modulus is getting increased with increase in the nylon 12 contents in the blends. Table III shows that elastic modulus increases from 18.2 to 59.2 MPa when the nylon 12 contents is raised from 0 to 25 wt %, corresponding to 225% increase in the elastic modulus. The increase in tensile modulus with increasing nylon 12 contents in the blends is attributed to more stiffness of nylon 12 phase as compared with elastomer phase. Tensile strength and elongation at break shows decreasing trend with increase in the nylon 12 content in the blends. The decrease in tensile strength with increasing nylon 12 contents is attributed to comparatively lower hydrogen bonding interactions (surface area) at the interfaces between the blended components because of increase in size of nylon 12 phase. Smaller the particle size of nylon 12, greater will be the surface area for hydrogen bonding interactions with the ATA-POE elastomer.[20] The decrease in tensile strength is rather modest up to 15 wt % of nylon 12 contents in the blends and then becomes greater at higher nylon 12 contents in the blends. Crisenza et al.[24] have also reported decrease in tensile strength and increase in modulus while working with chlorinated polyethylene/nylon terpolymer system in the low nylon content range.

The elastic recoverability of the samples is quantified in terms of tension set values and reported in Table III. Tension set shows increasing trend with increase in nylon 12 content in the blends. However, tension set of maximum 15% is obtained in

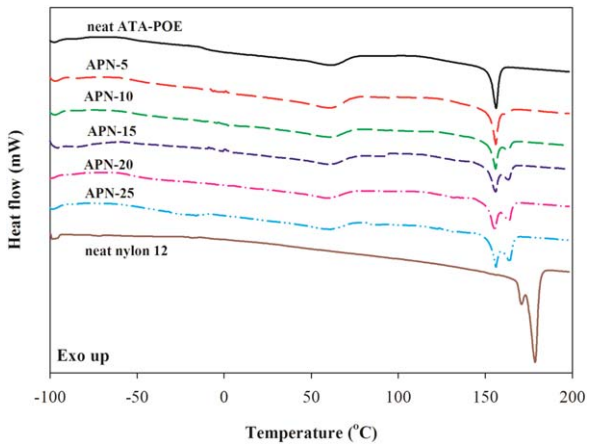

Figure 4. DSC thermograms for second heating of neat ATA-POE, neat nylon 12, and ATA-POE/nylon 12 blends. [Color figure can be viewed in the online issue, which is available at wileyonlinelibrary.com.]

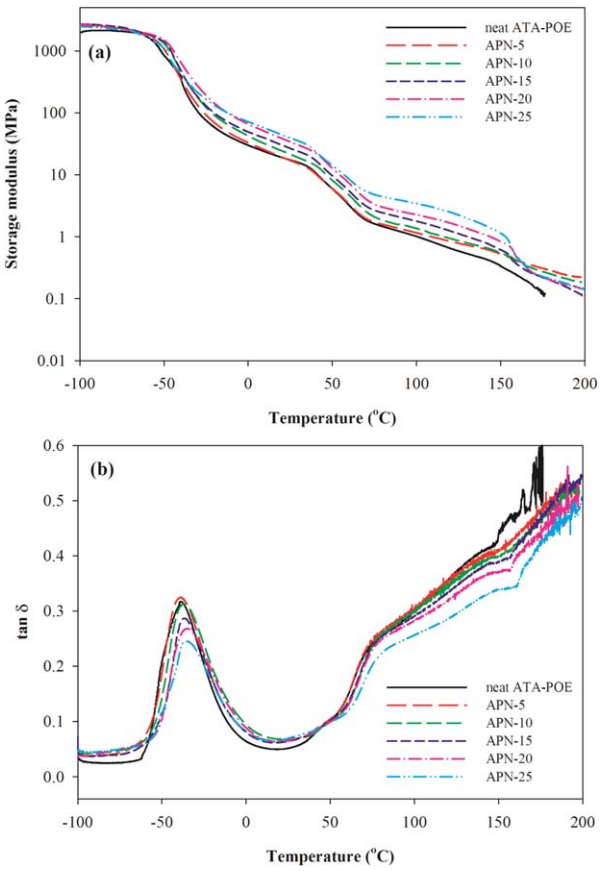

Figure 5. Variation in (a) storage moduli and (b) tan δ with temperature of neat ATA-POE and ATA-POE/nylon 12 blends. [Color figure can be viewed in the online issue, which is available at wileyonlinelibrary.com.]

Table II. Dynamic Mechanical Properties of the ATA-POE/Nylon 12 Blends

Sample	Nylon 12 (wt %)	E' at 30°C (Mpa)	E' at 50°C (Mpa)	E' at 100°C (Mpa)	T_g (°C)	Height of tan δ_{max}
Neat ATA-POE	0	15.55	5.89	1.01	−38.64	0.317
APN-5	5	15.07	6.04	1.16	−38.06	0.323
APN-10	10	18.77	8.05	1.36	−36.96	0.313
APN-15	15	23.73	9.76	1.79	−35.92	0.287
APN-20	20	30.03	12.55	2.27	−34.66	0.268
APN-25	25	35.03	14.13	3.42	−34.36	0.245

E' = Storage modulus, T_g= glass transition temperature of ATA-POE.

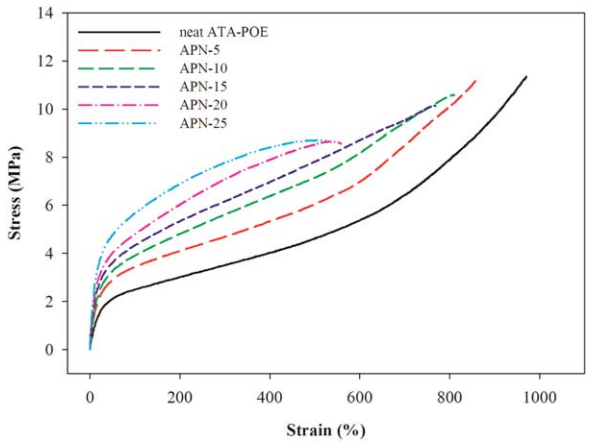

Figure 6. Tensile stress–strain curves of the neat ATA-POE and ATA-POE/nylon 12 blends. [Color figure can be viewed in the online issue, which is available at wileyonlinelibrary.com.]

the blend containing up to 25 wt % of nylon 12 contents which indicate that all the blends have good elastic recoverability.

Scratch Repairing Effect

Thermally triggered scratch healing behavior in the ATA-POE/nylon 12 blends was examined by using SEM and the results are shown in Figure 7. A scratch (60–70% of total thickness) was made on the surface of the samples with a razor blade. Figure 7(a) showed scratch width on the neat ATA-POE sample; similar scratch was made on the other blend samples. All the blend samples were heated at around 80°C in the convection oven for 5 min after being scratched. The blend samples containing up to 20 wt % of nylon 12 showed good scratch healing ability, as shown in Figure 7(C–F). The presence of dynamic supramolecular structure (ATA-POE) in the blends make them thermoresponsive[12] and the healing characteristic in the blend supports that amide group of nylon 12 participated in hydrogen bonding interactions with ATA-POE to some extent.[25] During scratching, temporary strain energy is stored in the polymer chains. Heating the scratched samples at 80°C (i.e., above the melting temperature of the elastomer phase) resulted in scratched surfaces to come close to each other to release temporary stored strain energy and the disruption of supramolecular structure. Heating above melting temperature also allows interfacial chain diffusion of low viscosity component across the interfaces and reforming of supramolecular hydrogen-bonded structure upon removal of heat.[26–28]

It is observed that when the nylon 12 content is 25 wt % [Figure 7(g)], the extent of healing decreases as compared with the blends with low nylon 12 contents. According to SEM analysis, particle size of the dispersed phase is growing with increasing nylon 12 contents in the blend. So, it is thought that larger particle size of dispersed phase (nylon 12) hinder the molecular mobility of the elastomer chains which resulted in poor healing of the blend.[29] Conclusively, the hydrogen bonding interactions between the blended components was used to enhance the mechanical properties, whereas thermoreversible supramolecular hydrogen bonded structure (ATA-POE) imparts thermal healing ability to the blend.

Furthermore, tensile testing experiments were conducted to quantify the healing efficiency[30] for the blend having 10 wt %

Table III. Tensile Properties of the ATA-POE/Nylon 12 Blends

Sample	Elastic modulus (Mpa)	50% tensile Modulus (Mpa)	300% tensile modulus (Mpa)	σ_b (Mpa)	ε_b (%)	Tension set (%)
Neat ATA-POE	18.2 ± 2.5	2.11 ± 0.02	3.51 ± 0.01	11.33 ± 0.38	970 ± 10	8.0
APN-5	29.9 ± 3.5	2.89 ± 0.02	4.69 ± 0.01	11.11 ± 0.82	880 ± 30	8.5
APN-10	35.7 ± 2.3	3.25 ± 0.03	5.61 ± 0.03	10.63 ± 0.62	817 ± 10	9.4
APN-15	49.3 ± 2.5	3.59 ± 0.02	6.41 ± 0.02	9.79 ± 0.43	749 ± 12	10.0
APN-20	53.3 ± 4.2	4.01 ± 0.02	7.11 ± 0.03	8.61 ± 0.87	585 ± 83	11.0
APN-25	59.2 ± 3.5	4.75 ± 0.01	7.77 ± 0.02	8.59 ± 0.39	483 ± 45	15.0

σ_b = Tensile strength; ε_b = Elongation at break.

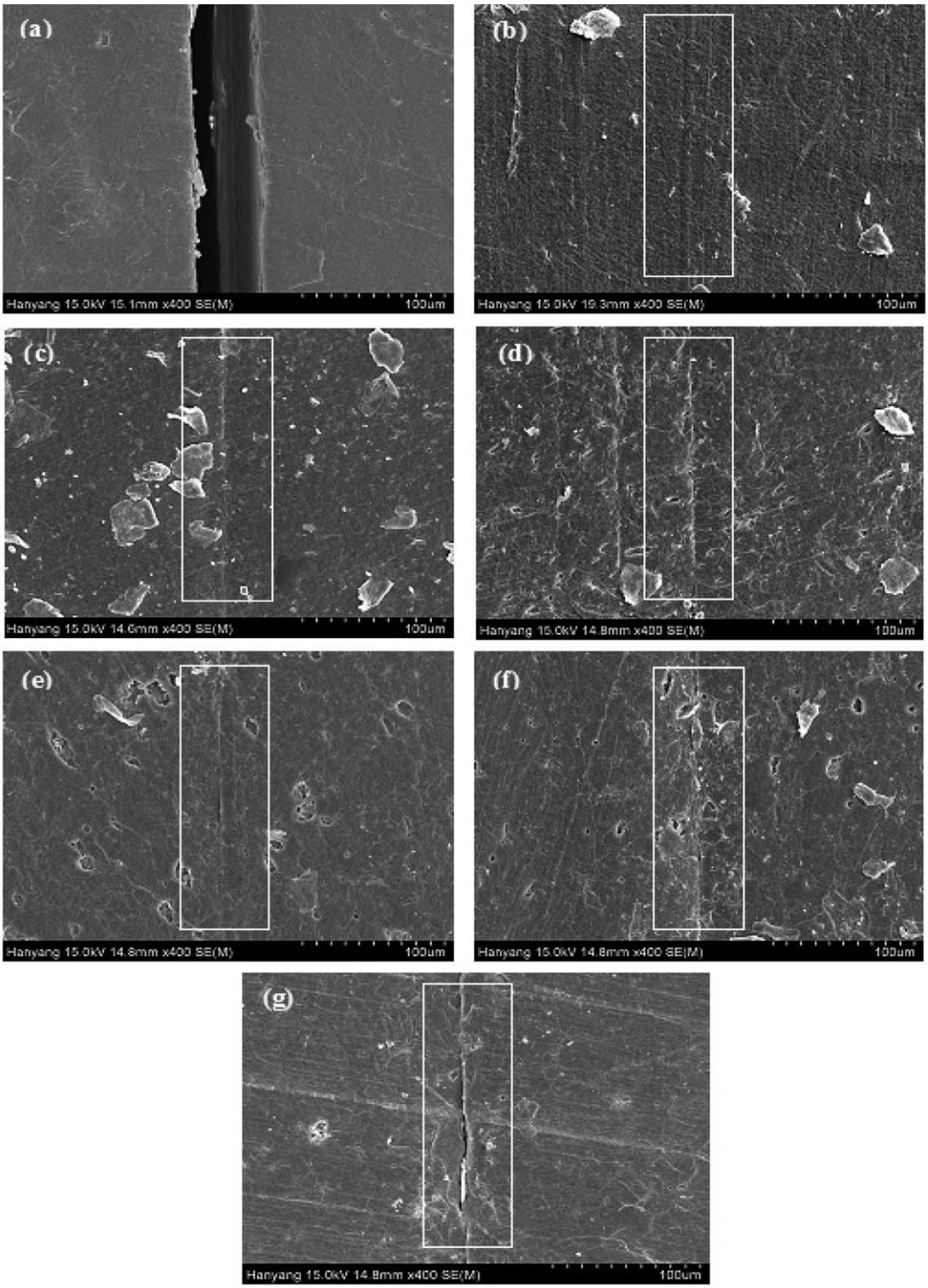

Figure 7. SEM micrographs of (a) the scratched sample width and the healed samples, (b) neat ATA-POE, (c) APN-5, (d) APN-10, (e) APN-15, (f) APN-20, and (g) APN-25.

nylon 12 contents and shown in Figure 8. A scratch (60–70% of total thickness) was marked on the dog-bone-shaped samples and the healing continued for 2 h at 90°C in the convection oven. At least, three samples were tested. Because of scratch on the surface, the tensile strength of the sample was significantly reduced to (3.21 ± 0.31) MPa and elongation at break reduced to (120 ± 28)%. The healed samples show tensile strength of (6.51 ± 0.25) MPa and the elongation at break of (518 ± 22)% for APN-10 sample, whereas original sample shows tensile strength of (10.63 ± 0.62) MPa and the elongation at break of

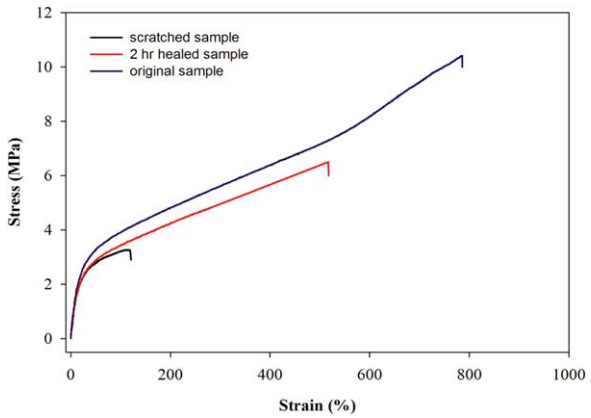

Figure 8. Stress–strain curves of scratched and thermally healed APN-10 blend sample. [Color figure can be viewed in the online issue, which is available at wileyonlinelibrary.com.]

(817 ± 10)% as shown in Table III. This reflects that most of the tensile strength (61%) and elongation at break (63%) recovered after thermal healing.

CONCLUSIONS

This article demonstrates that supramolecular thermally repairable elastomer (ATA-POE) can be reinforced with nylon 12 having fairly high elongation at break (>400%), while still maintaining its thermal healing ability. ATA-POE was formed by crosslinking of mPOE with ATA. The hydrogen bonding interactions between the blended components resulted in decrease of melting temperature of nylon 12 by 15°C as evidenced by DSC analysis. DMA and tensile testing showed improved storage modulus and tensile modulus, respectively, with increasing nylon 12 contents in the blends. All the blends also showed good elastic recoverability. The blends containing up to 20 wt % of nylon 12 showed good thermal healing ability. These unique supramolecular thermally repairable elastomers with enhanced mechanical properties may have potential applications in sport shields, automotive, and coating industry.

ACKNOWLEDGMENTS

Muhammad Kashif is highly thankful to Higher Education Commission (HEC) of Pakistan for research funding (PhD). This work is also supported by Fundamental R&D Program for Core Technology of Materials funded by Ministry of Knowledge Economy, Republic of Korea.

REFERENCES

1. Cazan, C.; Duta, A. Advances in Elastomers I; Springer, **2013**, p 183–228.
2. Costa, P.; Silvia, C.; Viana, J.; Lanceros Mendez, S. *Compos. Part B Eng.* **2014**, *57*, 242.
3. Roy, E.; Galas, J. C.; Veres, T. *Lab Chip* **2011**, *11*, 3193.
4. Aida, T.; Meijer, E. W.; Stupp, S. I. *Science* **2012**, *335*, 813.
5. Appel, W. P. J.; Portale, G.; Wisse, E.; Dankers, P. Y. W.; Meijer, E. W. *Macromolecules* **2011**, *44*, 6776.
6. Yang, L.; Lin, Y.; Wang, L.; Zhang, A. *Polym. Chem.* **2014**, *5*, 153.
7. Dong, J.; Weiss, R. *Macromol. Chem. Phys.* **2013**, *214*, 1238.
8. Kucera, L. R.; Brei, M. R.; Storey, R. F. *Polymer* **2013**, *54*, 3796.
9. Mora-Barrantes, I.; Malmierca, M. A.; Valentin, J. L.; Rodriguez, A.; Ibarra, L. *Soft Matter* **2012**, *8*, 5201.
10. Van der Mee, M.; l'Abee, R.; Portale, G.; Goossens, J.; Van Duin, M. *Macromolecules* **2008**, *41*, 5493.
11. Okada, O.; Keskkula, H.; Paul, D. *Polymer* **1999**, *40*, 2699.
12. Chino, K.; Ashiura, M. *Macromolecules* **2001**, *34*, 9201.
13. Chino, K. *KGK. Kautsch. Gummi Kunstst.* **2006**, *59*, 158.
14. Peng, C. C.; Abetz, V. *Macromolecules* **2005**, *38*, 5575.
15. Sun, C.; Van der Mee, M.; Goossens, J.; Van Duin, M. *Macromolecules* **2006**, *39*, 3441.
16. Chen, Y.; Kushner, A. M.; Williams, G. A.; Guan, Z. *Nat. Chem.* **2012**, *4*, 467.
17. Kashif, M.; Chang, Y. W. *Polym. Int.* **2014**. DOI: 10.1002/pi.4735.
18. González, L.; Ladegaard Skov, A.; Hvilsted, S. *J. Polym. Sci. Part A: Polym. Chem.* **2013**, *51*, 1359.
19. Hnilica, J.; Potočňáková, L.; Stupavská, M.; Kudrle, V. *Appl. Surf. Sci.* **2014**, *288*, 251.
20. Banerjee, S. S.; Bhowmick, A. K. *Polymer* **2013**, *54*, 6561.
21. Wu, C. S.; Liao, H. T.; Lai, S. M. *Polym. Plast. Technol. Eng.* **2002**, *41*, 645.
22. Gao, Q.; Scheinbeim, J. I. *Macromolecules* **2000**, *33*, 7564.
23. Li, Y.; Kaito, A. *Polymer* **2003**, *44*, 8167.
24. Crisenza, T.; Butt, H. J.; Koynov, K.; Simonutti, R. *Macromol. Rapid Commun.* **2012**, *33*, 114.
25. Khor, S. P.; Varley, R. J.; Shen, S. Z.; Yuan, Q. *J. Appl. Polym. Sci.* **2013**, *128*, 3743.
26. Herbst, F.; Döhler, D.; Michael, P.; Binder, W. H. *Macromol. Rapid Commun.* **2013**, *34*, 203.
27. Luo, X.; Mather, P. T. *ACS Macro Lett.* **2013**, *2*, 152.
28. Burattini, S.; Greenland, B. W.; Merino, D. H.; Weng, W.; Seppala, J.; Colquhoun, H. M.; Hayes, W.; Mackay, M. E.; Hamley, I. W.; Rowan, S. J. *J. Am. Chem. Soc.* **2010**, *132*, 12051.
29. Wang, C.; Liu, N.; Allen, R.; Tok, J. B. H.; Wu, Y.; Zhang, F.; Chen, Y.; Bao, Z. *Adv. Mater.* **2013**, *25*, 5785.
30. Bai, Y.; Chen, Y.; Wang, Q.; Wang, T. *J. Mater. Chem. A* **2014**, *2*, 9169.